Chapter 7

Results

7.1 Blinded results

The results for $\Delta P_\mu^\pi \xi$, the difference between $P_\mu^\pi \xi$ in data and a hidden simulation value, are shown in Table 7.1 and Fig. 7.1 for each data set. A weighted average over all the sets gives the result $+(77.4 \pm 2.0) \times 10^{-4}$ (confidence level of 46%). Sets 72, 76 and 86 are excluded since they have significantly larger polarisation systematic uncertainties. After including the other statistical and systematic uncertainties from Table 6.1 the result for $\Delta P_\mu^\pi \xi$ is

$$\Delta P_\mu^\pi \xi \;=\; \left[77.4 \pm 3.3\,(\text{stat.})^{+16.3}_{-8.2}\,(\text{syst.})\right] \times 10^{-4}. \tag{7.1}$$

This is a factor of 2.3 more precise that the previous TWIST measurement of $P_\mu^\pi \xi = 1.0003 \pm 0.0006\,(\text{stat.}) \pm 0.0038\,(\text{syst.})$[21], and a factor of 5.1 more precise than the pre-TWIST measurement of $P_\mu^\pi \xi = 1.0027 \pm 0.0079\,(\text{stat.}) \pm 0.0030\,(\text{syst.})$[67] that was described in Section 1.7.1.

The fit qualities in Table 7.1 are good. This is confirmed by examining the normalised fit residuals, which are shown for a nominal set in Fig. 7.2; there is no evidence of a dependence on momentum or $\cos\theta$, within the available statistics.

7.2 "White box" consistency test

The hidden simulation value of $P_\mu^\pi \xi$ will not be revealed until October 2009, meaning that the result for the data $P_\mu^\pi \xi$ is currently unknown. After the hidden $P_\mu^\pi \xi$ is revealed a "white box" consistency test will be carried out. Specifically a new simulation will be created with the measured $P_\mu^\pi \xi$ value, and this will be fit against the data; the consistency test is passed if a spectrum fit of the data to the new simulations finds no difference in $P_\mu^\pi \xi$; this would indicate that corrections have been applied with the correct sign.

Table 7.1: Difference between the data and a hidden simulation value of $P_\mu^\pi \xi$. The results have been averaged over the two energy calibration strategies in Section 6.8.2. The statistical spectrum fit uncertainties are shown. There are 2439 degrees of freedom. Sets 72, 76 and 86 are *not* used in the $P_\mu^\pi \xi$ result. The corrections are from production target scattering and the time dependent relaxation rate, as described in Section 6.2.

Set	Target	Description	$\Delta P_\mu^\pi \xi$ ($\times 10^{-4}$)		χ^2	Confidence
			Uncorrected	Corrected		
68	Ag	Stopping distrib. peaked $\frac{1}{3}$ into target	78.3	82.5 ± 6.9	2376	81.5
70	Ag	B = 1.96 T	71.2	75.4 ± 5.8	2426	57.2
71	Ag	B = 2.04 T	85.5	89.7 ± 6.1	2389	76.0
74	Ag	Nominal A	77.6	81.8 ± 6.9	2424	58.6
75	Ag	Nominal B	71.7	75.9 ± 5.9	2494	21.6
83	Al	Downstream beam package in place	73.9	79.3 ± 6.0	2376	81.5
84	Al	Nominal C	64.8	70.2 ± 6.3	2537	8.2
87	Al	Nominal D	71.9	77.3 ± 6.2	2442	48.1
91	Al	Lower momentum I	65.9	76.3 ± 11.0	2549	6.0
92	Al	Lower momentum II	62.5	72.2 ± 9.4	2475	29.9
93	Al	Lower momentum III	54.5	64.2 ± 7.8	2439	49.6
72	Ag	TECs-in, nominal beam	86.3	90.5 ± 6.0	2517	13.2
76	Ag	Steered beam A	30.1	34.3 ± 6.5	2415	63.4
86	Al	Steered beam B	51.3	56.7 ± 5.7	2419	60.9

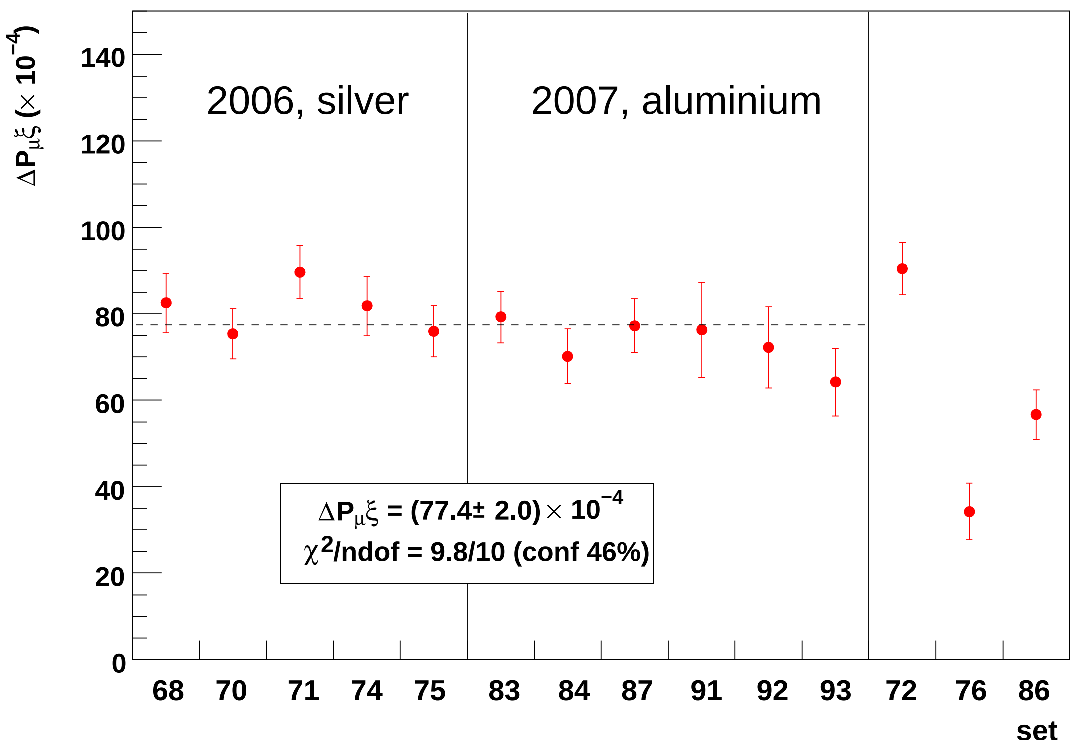

Figure 7.1: Consistency of $\Delta P_\mu^\pi \xi$, the difference in $P_\mu^\pi \xi$ between the data and a hidden value in the simulation. The uncertainties are statistical. Sets 72, 76 and 86 are not included in the $\Delta P_\mu^\pi \xi$ result due to their significantly larger P_μ systematic uncertainty.

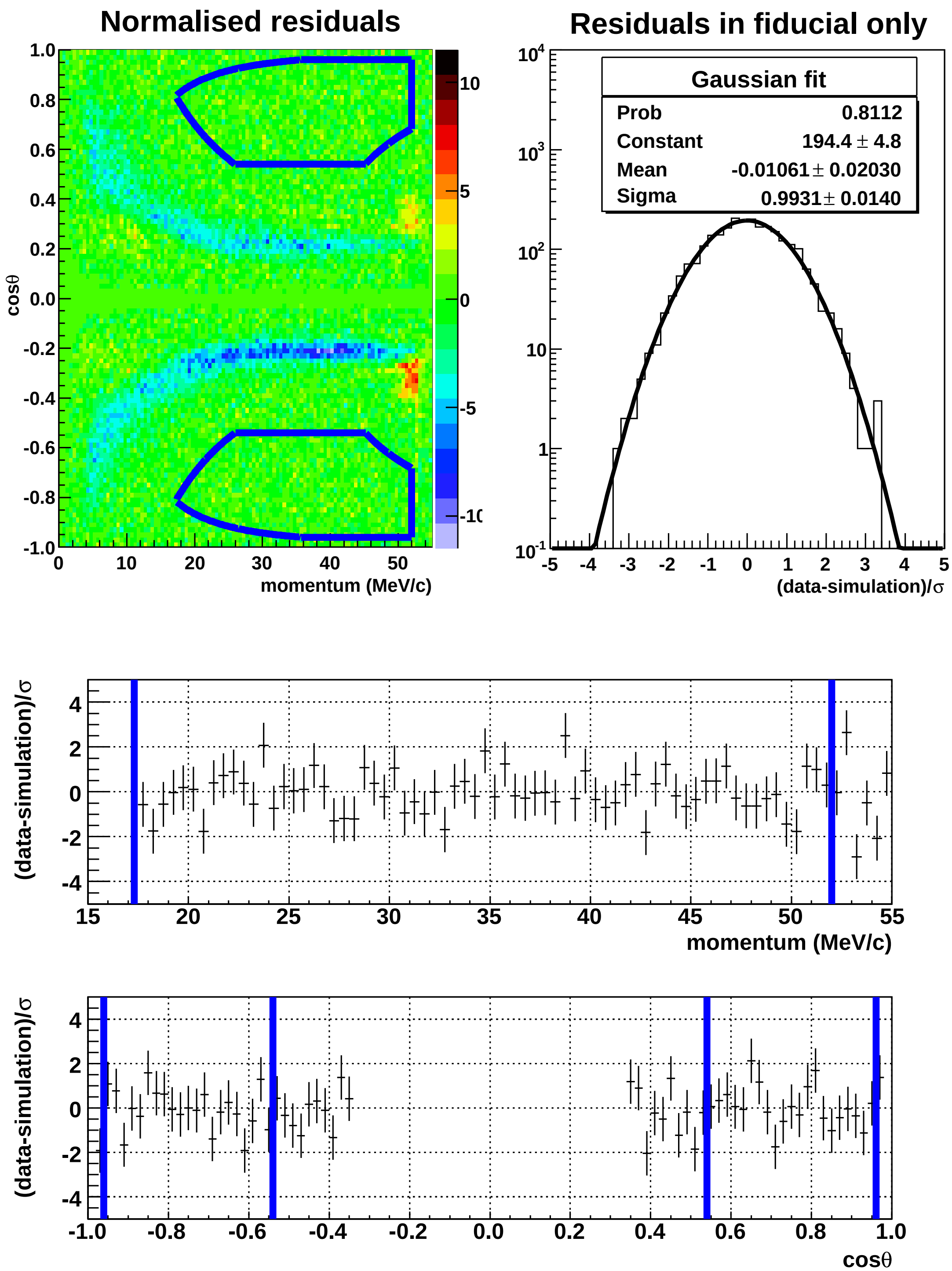

Figure 7.2: Normalised residuals from a spectrum fit of nominal data to its accompanying simulation. The thick blue lines indicate the kinematic fiducial boundaries. Within the fiducial region there is no evidence of structure.

7.3 Physics implications

7.3.1 Global analysis of muon decay data

The global analysis of muon decay data was described in Section 1.4.2. The two most recent analyses[7, 10] used the same software. The first analysis included the TWIST ρ and δ results from the 2002 datasets, and the second used the TWIST ρ and δ results from the 2004 datasets[46]. The same analysis software is now used to repeat the global analysis: $P_\mu^\pi \xi$ is assumed to be its standard model value of one, and ρ and δ are fixed to their values from Ref. [10]. The results are shown in Table 7.2, where the most significant changes are in the $|g^S_{RR}|$, $|g^V_{RR}|$, and $|g^V_{RR}|$ coupling constants. There will be further improvement when new ρ and δ results are completed using the same data as this measurement.

The global analysis also gives limits on the probability of a right-handed muon decaying into a left or right-handed electron (see Eq. (1.24)). This is forbidden in the standard model, and prior to TWIST the 90% upper limit on the decay probability was 1.4%. This was reduced to 0.23% in Ref. [10], and is now further reduced to 0.20% using the current $P_\mu^\pi \xi$ measurement.

Table 7.2: 90% confidence limits on the weak coupling constants. Limits on $|g^S_{LL}|$ and $|g^V_{LL}|$ are from Ref. [3].

	Prior to TWIST[9]	TWIST results using 2004 data[10]	This measurement of $P_\mu^\pi \xi$, ρ and δ from [10]
$\lvert g^S_{RR}\rvert$	< 0.066	< 0.062	< 0.057
$\lvert g^V_{RR}\rvert$	< 0.033	< 0.031	< 0.028
$\lvert g^S_{LR}\rvert$	< 0.125	< 0.074	< 0.069
$\lvert g^V_{LR}\rvert$	< 0.060	< 0.025	< 0.024
$\lvert g^T_{LR}\rvert$	< 0.036	< 0.021	< 0.020
$\lvert g^S_{RL}\rvert$	< 0.424	< 0.412	< 0.414
$\lvert g^V_{RL}\rvert$	< 0.110	< 0.104	< 0.103
$\lvert g^T_{RL}\rvert$	< 0.122	< 0.103	< 0.103
$\lvert g^S_{LL}\rvert$	< 0.550	< 0.550	< 0.550
$\lvert g^V_{LL}\rvert$	> 0.960	> 0.960	> 0.960

[46] The previous TWIST $P_\mu^\pi \xi$ result was included in the latest global analysis, but it had no effect since a more stringent limit of $P_\mu \xi \delta/\rho > 0.99682$ (90% C.L.) existed[29, 30].

7.3.2 Left-right symmetric models

Several left-right symmetric (LRS) models were described in Section 1.5.2. The most general form of the weak interaction allows $\xi > 1$, but LRS models require that $P_\mu^\pi \xi \leq 1$. Therefore if $P_\mu^\pi \xi$ is equal to the standard model value of one, the lower uncertainty on the current measurement (8.2×10^{-4}) can be used to exclude values of $(g_L/g_R)m_2$ and ζ using Eqs. (1.26)-(1.31) (ζ is the mixing angle between the left and right-handed W-boson eigenstates, g_L and g_R are the weak coupling constants for the predominantly left and right-handed W-bosons, and m_2 is the mass of the predominantly right-handed W-boson). The substantially improved exclusion region (90% confidence limit) is shown in Fig. 7.3.

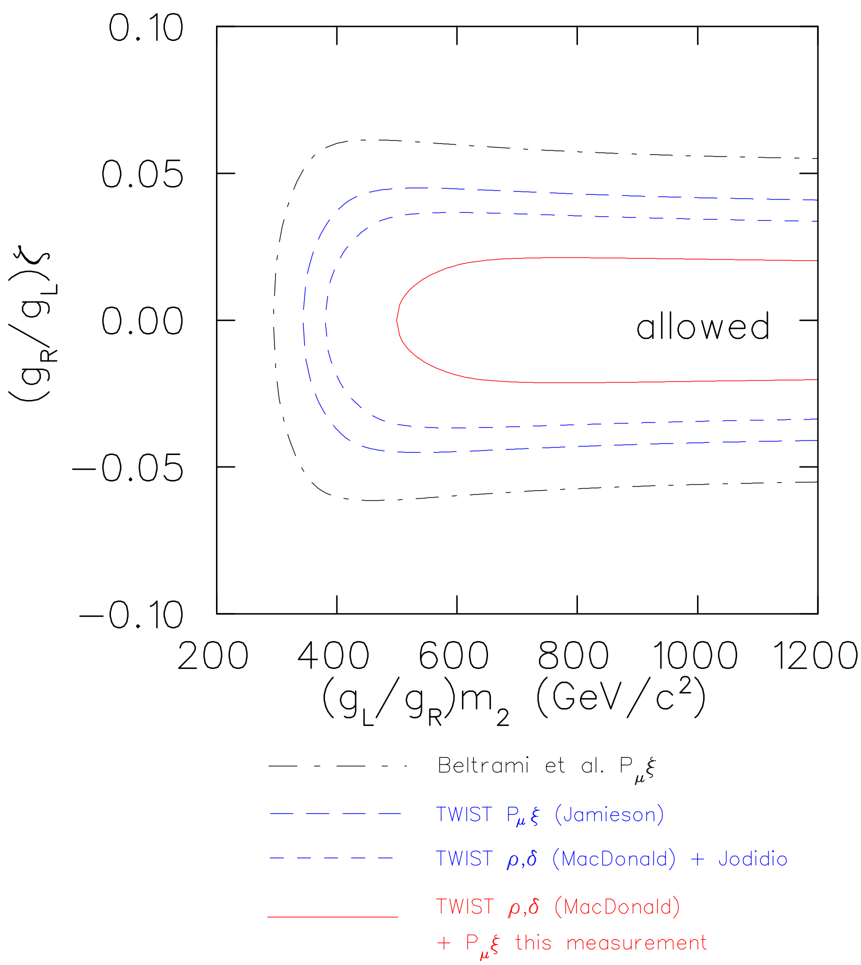

Figure 7.3: Exclusion region (90% confidence limit) for ζ and $(g_L/g_R)m_2$, which are defined in the text. Beltrami refers to the pre-TWIST $P_\mu^\pi \xi$ measurement[67]. Jamieson is the previous TWIST direct $P_\mu^\pi \xi$ value[21]. MacDonald is the ρ and δ measurements from the TWIST 2004 datasets[10]. Jodidio refers to the limit of $P_\mu \xi \delta/\rho > 0.99682$ (90% C.L.) from Refs. [29, 30].

7.4 Future experiments

A $P_\mu^\pi \xi$ measurement with an order of magnitude improvement is potentially possible with a TWIST-style experiment (*i.e* longitudinally polarised muons delivered into the centre of uniform magnetic field, with high precision positron tracking). Suggestions and consideriations will now be given for each of the uncertainties from the current measurement.

7.4.1 Statistical uncertainty

The statistical uncertainty for this measurement is already at the level of 3.3×10^{-4}, or just 2.0×10^{-4} for the part that originates from the decay spectrum fit. This was achieved with about four months of continuous data acquisition at a surface muon rate rate of $2000 - 5000\,\mathrm{s}^{-1}$ (a significant amount of tuning over the years 2000 to 2006 was necessary to achieve the required beam quality). The statistical uncertainty of a future measurement could be reduced to acceptable levels by using a channel with an order of magnitude higher flux. For example, a new μE4 channel at PSI already achieves this by placing radiation-hard solenoids close to the production target, allowing an acceptance of $\Delta\Omega \sim 135\,\mathrm{msr}$[80] compared to 29 msr from the M13 beam line. If the TWIST analysis approach were adopted, using an accompanying simulation to include inefficiences and biases, then the simulation statistics could be significantly increased by taking advantage of faster CPUs.

7.4.2 Magnetic field map uncertainty

The dominant systematic uncertainty from the fringe field could be reduced. We used an MRI magnet surrounded by a custom steel yoke, but a specially constructed magnet could provide a more gradual fringe field by increasing the z-distance over which the field reaches its full strength. Alternatively a higher rate muon channel would allow the possibility of beam collimation; by selecting low angle muons that undergo very little depolarisation, the uncertainty on that depolarisation will be decreased. However, such collimators could introduce an additional uncertainty from muons scattering off them, and this would have to be carefully assessed.

The measurement of our magnetic field could have been done better. A future experiment would need alignments of the measuring apparatus under control at the $< 0.5\,\mathrm{cm}$ and $< 1\,\mathrm{mrad}$ level, and must measure all three components of the magnetic field. This last point cannot be stressed enough. Also, the current experiment would have benefited from field measurements at finer space intervals (in all coordinates) over the region that the muons actually passed through.

We used the OPERA magnetic field simulation to produce the B_x and B_y components of our field map. With all three components measured, it may be unncessary to have a magnetic field simulation at all. However, if a simulation is required, it is recommended that more than one piece of software is used; for example, the latest version of OPERA[83], or the COMSOL Multiphysics (formerly FEMLAB) software[101].

The TWIST approach was to measure the muons before the fringe field, and rely on a GEANT3 simulation to predict the final polarisation. There are at least two ways to improve the confidence in the final polarisation: first the spin could be transported by one or more independent simulations; second the beam could be steered off-axis in order to lower the polarisation, and a simulation's ability to reproduce the polarisation change from the data would allow confidence to be gained. As seen in this thesis, the alignment of the beam and field must be under strict control in order for the second approach to work.

The time expansion chambers (TECs) that measured our muon beam had adequate precision, but suffered from alignment uncertainties and aging problems that would be more significant for a future measurement. An improved measurement using a similar device would have to address these issues. A significant uncertainty from the TECs originated from the simulation's ability to correct for the multiple scattering that takes place while the muons pass through the active volume; a subsidiary experiment may be needed to validate the simulation's accuracy in making this correction.

An alternative is to measure the muon beam inside the strong magnetic field. This would present a greater engineering and analysis challenge, since the device would have to work in a strong magnetic field and the reconstructed trajectories would be helices. If carried out accurately, this approach has the potential to eliminate many of the problems with simulating the spin.

7.4.3 Stopping material depolarisation uncertainty

For the current measurement the polarisation's relaxation rate was measured using the normal data. A subsidiary μ^+SR experiment provided a consistent but uncompetitive result. A future experiment should consider an integrated "μ^+SR mode", with a higher beam intensity and a simple analysis that only identifies particles and their times. The goal should be to unequivocally determine the form of $P_\mu(t)$ and its parameters. Since this experimental mode would not measure the absolute polarisation, a spin rotator should be considered to significantly reduce beam positrons, which would allow a much higher muon rate. (A μ^+SR analysis was considered using the existing TWIST detector. The proportional chambers

(PCs) had a timing resolution of $\sim 20\,\text{ns}$, and could identify particles based on their pulse width. This would have allowed us to use decay data below $1\,\mu\text{s}$ to better determine the relaxation rate.)

If a "μ^+SR mode" is not possible, then a subsidary μ^+SR experiment should be considered from the outset. Suggestions are made in Section H.9 that would allow a better time differential μ^+SR measurement. Another useful measurement could be provided by a pulsed muon setup such as the Rutherford Appleton Laboratory (UK).

For the TWIST polarisation measurements, only aluminium and silver targets were used. Additional targets that produced consistent $P_\mu^\pi \xi$ measurements would strengthen a future result.

We were able to successfully eliminate muons that stopped in the gas before our stopping target; a stricter cut could have further reduced the contamination, with a loss of statistical precision. However, one surprise was our simulation's prediction that 0.2% of muons passed through the metal stopping target and entered PC7, but did not have enough energy to produce a signal. This could have been reduced by also running the PCs after the target at a lower voltage in order to increase their sensitivity to muons.

7.4.4 Other uncertainties

The uncertainty from production target scattering can be reduced in three ways: first by selecting a smaller momentum resolution, which would be feasible with a higher intensity beamline. Second, by a more accurate validation of the multiple scattering within the simulation. Third, if there was more control over the range of surface muons, then a significantly lower momentum muon beam could be selected that corresponds to muons from much deeper in the production target; the difference in polarisation between the lower momentum muons and surface muons would then help to validate a simulation of multiple scattering.

There are theoretical considerations at the $< 1 \times 10^{-4}$ level that would be important for future measurements. The next level of radiative corrections (full $O(\alpha^3)$) would ideally be evaluated. A calculation of radiative corrections that does not assume an underlying $(V - A)$ interaction would be very welcome. The pion radiative decay mode should also be considered more carefully; such calculations have been carried out for the purposes of TWIST[102].

The inefficiency and resolution were both measured here using a special analysis with the muons stopped at the entrance of the spectrometer, and the decay positron reconstructed separately in each half. A future experiment should consider designing the beam line to allow a "spread muon tune", where the muons stop close to the detector entrance but spreadout over a much wider area than usual. In addition, the stopping target should be as large as possible to allow a wide range of decay positron phase space to be reconstructed in each detector half. Also the ability to rotate the entire detector (*i.e.* swap the usptream and downstream ends) would provide a more stringent test of measurements that compare the upstream and downstream response of the detector.

The uncertainties from positron interactions (mostly δ-electrons and bremsstrahlung) will need careful consideration. This may require work by theorists, or a comparison of several simulations that claim to accurately reproduce these processes in the relevant energy range. A future experimenter should consider a subsidiary experiment to help understand these processes better in the low energy range.

Another area requiring thought is the energy calibration. Inevitably a correction or calibration will be needed since the decay positron construction will have subtle biases and systematic errors. The method of measuring and then propagating such a correction will likely be dominant in a future $P_\mu^\pi \xi$ measurement. For the TWIST experiment this correction was due to a complex combination of errors in the magnetic field map, imperfect drift cell space-time-relationships, bias from the helix fitting, the energy-loss model in the simulation, multiple scattering of the decay positron and uncertainties in the stopping distribution; these pieces could not be disentangled, and as a result a conservative approach was taken to the propagation of the energy calibration to the bulk of the decay spectrum. A future experiment must consider ways of eliminating these errors, or breaking them into orthogonal pieces; see Ref. [100] for more information.

The remaining uncertainties from Table 6.1 could have easily been reduced. The beam intensity uncertainty could be eliminated by tuning the simulation's muon rate to properly match the data, using the R_μ criteria described in Section 6.3.6. The uncertainty from background muons could be reduced by tuning the stopping distribution based on the $\alpha_{\text{diff.}}$ criteria in Section 6.3.5, and/or adding to the simulation a source of pions at the end of the M13 beam line. The refined space-time-relationships in the DCs and the wire time offsets were already adequate for a measurement at the $< 0.5 \times 10^{-4}$ level. The foil bulge uncertainty could have been reduced by cutting the data more strictly to remove all periods where a rapid change in ambient temperature or pressure occurred; the evaluation here is already an upper limit. The strict engineering requirements of the TWIST detector meant that alignment uncertainties were already at a negligible level. The outside material systematic could be eliminated by adding more active materials to the simulation, so that it matched the data better. The η correlation will be reduced for future measurements after a global analysis using this $P_\mu^\pi \xi$ measurement and the simultaneous ρ and δ measurements.

In addition to the goal of extracting $P_\mu^\pi \xi$ (and ρ, δ), a future experiment should consider subsidiary measurements that may even benefit the main experiment. An η measurement from the decay spectrum would provide a validation of the results that use the transverse polarisation of the decay positron, although positron interactions would have to be thoroughly understood since η affects the low momentum end of the spectrum. Some extensions to the standard model postulate additional parameters to describe the decay spectrum; see Ref. [89] for a more detailed discussion. The *negative* muon decay spectrum for each stopping target could be produced using the same analysis software; see Ref. [103] for such a measurement (the first of its kind) that used the TWIST apparatus. Lastly, if there was a possiblity to switch between muons sourced from pions and kaons, then the resulting $P_\mu^\pi \xi$ and $P_\mu^K \xi$ measurements would provide a more complete test of the standard model.

7.5 Conclusions

The quantity $\Delta P_\mu^\pi \xi$, the difference between $P_\mu^\pi \xi$ and a hidden simulation value, is measured as

$$\Delta P_\mu^\pi \xi \ = \left[77.4 \pm 3.3\,(\text{stat.})^{+16.3}_{-8.2}\,(\text{syst.})\right] \times 10^{-4}. \tag{7.2}$$

This is the final direct $P_\mu^\pi \xi$ measurement from the TWIST collaboration, and is a factor of 5.1 more precise that the pre-TWIST result[67]. This measurement's accuracy is limited by a systematic uncertainty from predicting P_μ at the time of decay; this was caused by our poor knowledge of the transversrse magnetic field components that were used to transport the spin in the simulation. This result improves the limits on the mixing angle in left-right symmetric models, and reduces the limits on extensions to the standard model, as part of a global analysis including new results for ρ and δ.

Bibliography

[1] S. Weinberg. A Model of Leptons. *Phys. Rev. Lett.*, 19(21):1264–1266, Nov 1967.

[2] Donald Hill Perkins. *Introduction to High-Energy Physics; 4th ed.* Cambridge Univ. Press, Cambridge, 2000.

[3] C. Amsler *et al.* Review of Particle Physics. *Phys. Lett. B*, 667(1-5):1–6, 2008. Review of Particle Physics.

[4] D. Griffiths. *Introduction to Elementary Particles.* Wiley, 1987.

[5] M. Goldhaber, L. Grodzins, and A. W. Sunyar. Helicity of Neutrinos. *Phys. Rev.*, 109:1015 – 1017, 1958.

[6] D. Binosi and L. Theuβl. JaxoDraw: A graphical user interface for drawing Feynman diagrams. *Comput. Phys. Commun.*, 161:76–86, August 2004.

[7] C.A. Gagliardi, R.E. Tribble and N.J. Williams. Global analysis of muon decay measurements. *Phys. Rev. D*, 72(7):073002, Oct 2005.

[8] W. Fetscher, H.-J. Gerber and K.F. Johnson. Muon decay: complete determination of the interaction and comparison with the standard model. *Phys. Lett. B*, 173(1):102–106, 1986.

[9] S. Eidelman *et al.* Review of Particle Physics. *Phys. Lett. B*, 592(1-4):1–5, 2004. Review of Particle Physics.

[10] R.P. MacDonald *et al.* Precision measurement of the muon decay parameters ρ and δ. *Phys. Rev. D*, 78(3):032010, 2008.

[11] A. Sirlin, New York University, USA. Private communication.

[12] A. B. Arbuzov. First-order radiative corrections to polarized muon decay spectrum. *Phys. Lett. B*, 524(1-2):99 – 106, 2002.

[13] A. Arbuzov, A. Czarnecki and A. Gaponenko. Muon decay spectrum: Leading logarithmic approximation. *Phys. Rev. D*, 65:113006, 2002.

[14] A. Arbuzov and K. Melnikov. $\mathcal{O}(\alpha^2 \ln(m_\mu/m_e))$ corrections to electron energy spectrum in muon decay. *Phys. Rev. D*, 66:093003, 2002.

[15] A. Arbuzov. Higher order QED corrections to muon decay spectrum. *J. High Energy Phys.*, 2003(03):063–063, 2003.

[16] K. Melnikov C. Anastasiou and F. Petriello. The electron energy spectrum in muon decay through $\mathcal{O}(\alpha^2)$. *J. High Energy Phys.*, (09):014, 2007.

[17] N. Danneberg *et al.* Muon Decay: Measurement of the Transverse Polarization of the Decay Positrons and its Implications for the Fermi Coupling Constant and Time Reversal Invariance. *Phys. Rev. Lett.*, 94:021802, 2005.

[18] R.P. MacDonald. *A Precision Measurement of the Muon Decay Parameters ρ and δ.* PhD thesis, University of Alberta, 2008.

[19] P. Herczeg. On muon decay in left-right-symmetric electroweak models. *Phys. Rev. D*, 34(11):3449–3456, Dec 1986.

[20] V.M. Abazon *et al.* Search for W' Bosons Decaying to an Electron and a Neutrino with the D0 Detector. *Phys. Rev. Lett.*, 100:031804, 2008.

[21] B. Jamieson *et al.* Measurement of $P_\mu\xi$ in polarized muon decay. *Phys. Rev. D*, 74(7):072007, 2006.

[22] J.D. Jackson. *Classical Electrodynamics.* John Wiley & Sons, 1999.

[23] V. Bargmann, L. Michel and V.L. Telegdi. Precession of the Polarization of Particles Moving in a Homogeneous Electromagnetic Field. *Phys. Rev. Lett.*, 2:435–436, 1959.

[24] A. Balakin, V. Kurbanova and W. Zimdahl. Precession of a particle with anomalous magnetic moment in electromagnetic and gravitational pp-wave fields. *Gravity Cosmology Supplement*, 82:6–9, 2002.

[25] P. Depommier. The BMT equation. Presentation to TWIST collaboration, May 2006.

[26] P. Depommier. Muon depolarization in multiple scattering (TN100). Technical report, TWIST collaboration, TRIUMF, 2005.

[27] W.H. Koppenol. Names for muonium and hydrogen atoms and their ions(IUPAC Recommendations 2001). *Pure Appl. Chem.*, 73:377–379, 2001.

[28] M. Senba. Muon spin depolarization in noble gases during slowing down in a longitudinal magnetic field. *J. Phys. B: At. Mol. Opt. Phys.*, 31:5233–5260, 1998.

[29] A. Jodidio *et al.* Search for right-handed currents in muon decay. *Phys. Rev. D*, 34(7), 1986.

[30] A. Jodidio *et al.* Erratum: Search for right-handed currents in muon decay. *Phys. Rev. D*, 37(1), 1988.

[31] J. H. Brewer. Muon spin rotation/relaxation/resonance. In *Encyclopedia of Applied Physics 11*, pages 23–53. 1994.

[32] S.F.J. Cox. Implanted muon studies in condensed matter science. *J. Phys. C: Solid State Phys*, 20:3187–3319, 1987.

[33] O. Hartmann *et al.* Diffusion of positive muons in some cubic metals. *Phys. Lett. A*, 61(2):141 – 142, 1977.

[34] J. Brewer, University of British Columbia, Canada. Private communication.

[35] W.B. Gauster *et al.* Measurement of the depolarization rate of positive muons in copper and aluminum. *Solid State Commun.*, 24(9):619–622, 1977.

[36] W. Schilling. The physics of radiation damage in metals. *Hyperfine Interact.*, 4:636–644, 1978.

[37] D.K. Brice. Lattice atom displacements produced near the end of implanted μ^+ tracks. *Phys. Lett. A*, 66:53–56, 1978.

[38] P. Dalmas de Réotier and A. Yaouanc. Muon spin rotation and relaxation in magnetic materials. *J.Phys: Condens. Matter*, 9:9113–9166, 1997.

[39] P. Dalmas de Réotier and A. Yaouanc. Quantum calculation of the muon depolarization function: effect of spin dynamics in nuclear dipole systems. *J.Phys: Condens. Matter*, 4:4533–4556, 1992.

[40] A. Abragam. *Principles of Nuclear Magnetism.* International series of monographs on physics. Oxford University Press, 1986.

[41] R.S. Hayano *et al.* Zero- and low-field spin relaxation studied by positive muons. *Phys. Rev. B*, 20:850, 1979.

[42] W.J. Kossler *et al.* Diffusion and Trapping of Positive Muons in Al:Cu Alloys and in Deformed Al. *Phys. Rev. Lett.*, 41:1558–1561, 1978.

[43] O. Hartmann *et al.* Coherent Propagation and Strain-Induced Localization of Muons in Al. *Phys. Rev. Lett.*, 41:1055–1058, 1978.

[44] K.W. Kehr *et al.* Muon diffusion and trapping in aluminum and dilute aluminum alloys: Experiments and comparison with small-polaron theory. *Phys. Rev. B*, 26:567–589, 1982.

[45] K.W. Kehr. Empirical information on quantum diffusion. *Hyperfine Interact.*, 17-19:63–74, 1984.

[46] O. Hartmann. Diffusion and trapping of muons in aluminum: New experiments and comparison with Kondo theory. *Phys. Rev. B*, 37:4425–4440, 1988.

[47] O. Hartmann. New results on diffusion in fcc metals. *Hyperfine Interact.*, 64:641–648, 1990.

[48] O. Hartmann *et al.* Studies of μ^+ Localization in Cu, Al, and Al alloys in the Temperature Interval $0.03 - 100\,\mathrm{K}$. *Phys. Rev. Lett.*, 44:337–340, 1980.

[49] D.P. Stoker *et al.* Search for Right-Handed Currents by Means of Muon Spin Rotation. *Phys. Rev. Lett.*, 54:1887–1890, 1985.

[50] D.P. Stoker, University of California, Irvine, USA. Private communication.

[51] J. Korringa. Nuclear magnetic relaxation and resonance (sic.) line shift in metals. *Physica*, 7-8:601–610, 1950.

[52] S.J. Blundell and S.F.J. Cox. Longitudinal muon spin relaxation in metals and semimetals and the Korringa law. *J. Phys.: Condens. Matter*, 13:2163–2168, 2001.

[53] J.H. Brewer *et al.* *Positive muons and muonium in matter.* Muon Physics. Academic Press Inc (London) Limited, 1975.

[54] S.F.J. Cox *et al.* Muon Korringa relaxation. *Physica B*, 289-290:594–597, 2000.

[55] R.H. Heffner. Muon spin depolarization in nonmagnetic metals doped with paramagnetic impurities. *Hyperfine Interact.*, 8:655–662, 1981.

[56] J.A. Brown *et al.* Muon Depolarization by Paramagnetic Impurities in Nonmagnetic Metals. *Phys. Rev. Lett.*, 47:261–264, 1981.

[57] B. Jamieson. *Measurement of the muon decay asymmetry parameter with the TWIST spectrometer*. PhD thesis, University of British Columbia, 2006.

[58] T.D. Lee and C.N. Yang. Question of Parity Conservation in Weak Interactions. *Phys. Rev.*, 104(1):254–258, Oct 1956.

[59] ARGUS collaboration. Determination of the Michel Parameters ρ, ξ, and δ in τ-Lepton Decays with $\tau \to \rho\nu$ Tags. *Phys. Lett. B*, 431:179–187, 1998.

[60] L3 Collaboration. Measurement of the Michel parameters and the average tau-neutrino helicity from tau decays at LEP. *Phys. Lett. B*, 438:405–416, 1998.

[61] R. Bartoldus. Measurements of the Michel Parameters in Leptonic Tau Decays using the OPAL Detector at LEP. *Nucl. Phys. B (Proc. Suppl.)*, 76:147–157, 1999.

[62] R.L. Garwin, L.M. Lederman and M. Weinrich. Observations of the Failure of Conservation of Parity and Charge Conjugation in Meson Decays: the Magnetic Moment of the Free Muon. *Phys. Rev.*, 105:1415, January 1957.

[63] G. R. Lynch, J. Orear, and S. Rosendorff. Muon decay in nuclear emulsion at 25 000 gauss. *Phys. Rev.*, 120(6):2277, Dec 1960.

[64] M. Bardon, D. Berley, and L. M. Lederman. Asymmetry parameter in muon decay. *Phys. Rev. Lett.*, 2(2):56–57, Jan 1959.

[65] Richard J. Plano. Momentum and asymmetry spectrum of μ-meson decay. *Phys. Rev.*, 119(4):1400–1408, Aug 1960.

[66] Akhmanov *et al. Sov. J. Nucl. Phys*, 6:230, 1968.

[67] I. Beltrami *et al.* Muon decay: Measurement of the integral asymmetry parameter. *Phys. Lett. B*, 194(2):326–330, 1987.

[68] Ali-Zade *et al. Soviet Phys.-JETP*, 36 (9):940, 1959.

[69] R.S. Hayano *et al.* Search for Right-Handed Currents in the Decay $K^+ \to \mu^+\nu$. *Phys. Rev. Lett.*, 52(5):329–332, Jan 1984.

[70] J. Imazato *et al.* Search for right-handed currents in the decay chain $K^+ \to \mu^+\nu$, $\mu^+ \to e + \nu\bar{\nu}$. *Phys. Rev. Lett.*, 69(6):877–880, Aug 1992.

[71] T. Yamanaka *et al.* Search for right-handed currents in the decay $K^+ \to \mu^+\nu$. *Phys. Rev. D*, 34(1):85–96, Jul 1986.

[72] C.A. Coombes *et al.* Polarization of μ^+ Mesons from the Decay of K^+ Mesons. *Phys. Rev.*, 108(5):1348–1351, Dec 1957.

[73] D. Cutts, T. Elioff, and R. Stiening. Muon Polarization and Energy Spectrum in $K^+ \to \pi^0 + \mu^+ + \nu$. *Phys. Rev.*, 138(4B):B969–B979, May 1965.

[74] D. Cutts, R. Stiening, C. Wiegand, and M. Deutsch. Measurement of the Muon Polarization Vector in $K^+ \to \pi^0 + \mu^+ + \nu$. *Phys. Rev.*, 184(5):1380–1392, Aug 1969.

[75] R.S. Henderson *et al.* Precision planar drift chambers and cradle for the TWIST muon decay spectrometer. *Nucl. Instrum. Methods Phys. Res., Sect. A*, 548:306–335, August 2005.

[76] J. Hu *et al.* Time expansion chamber system for characterization of TWIST low-energy muon beams. *Nucl. Instrum. Methods Phys. Res., Sect. A*, 566:563–574, October 2006.

[77] C.J. Oram, J.B. Warren and G.M. Marshall. Commissioning of a new low energy $\pi - \mu$ channel at TRIUMF. *Nucl. Instrum. Methods*, 179:95–103, January 1981.

[78] J. Doornbos. The tuning of M13 for TWIST, theory and some results. Internal TWIST bulletin boards, December 2000.

[79] R.E. Mischke, TRIUMF, Vancouver, Canada. Private communication.

[80] T. Prokscha et al. The new μE4 beam at PSI: A hybrid-type large acceptance channel for the generation of a high intensity surface-muon beam. *Nucl. Instrum. Methods Phys. Res., Sect. A*, 595.

[81] J.E. Draper. Beam Steering with Quadrupole and with Rectangular Box Magnets. *Rev. Sci. Instrum.*, 37:1390, October 1966.

[82] J. Musser. *Measurement of the Michel parameter ρ in muon decay.* PhD thesis, Texas A&M University, 2005.

[83] Vector Fields. OPERA 3D simulation software. http://vectorfields.com.

[84] G.M. Marshall, TRIUMF, Vancouver, Canada. Private communication.

[85] A. Gaponenko. *A Precision Measurement of the Muon Decay Parameter δ*. PhD thesis, University of Alberta, 2005.

[86] D. Wright. TN1: DME / He WC Gas Comparison. Technical report, TWIST collaboration, TRIUMF, October 1996.

[87] LeCroy Corporation. 1877 Multihit Time-to-Digital Converter: Specification. `http://www.lecroy.com/lrs/dsheets/1877.htm`.

[88] LeCroy Corporation. LeCroy 1877 Fastbus TDC Manual.

[89] A. Hillairet. *Measurement of δ (in preparation)*. PhD thesis, University of Victoria, 2009.

[90] R. Brun and F. Rademakers. ROOT - An Object Oriented Data Analysis Framework. *Nucl. Inst. & Meth. in Phys. Res. A*, 389:81–86, 1997.

[91] R. Brun *et al.* `GEANT`, version 3.2114.

[92] F. James. Fitting tracks in wire chambers using the Chebyshev norm instead of least squares. *Nucl. Instrum. Methods Phys. Res.*, 211(1):145 – 152, 1983.

[93] R. Veenhof. Garfield - simulation of gaseous detectors. CERN Program Library W5050.

[94] C. Gagliardi, Texas A&M University, Texas, USA. Private communication.

[95] P. Depommier. TN49: Muon polarisation in electromagnetic fields. Technical report, TWIST collaboration, TRIUMF, 2001.

[96] R. Openshaw, TRIUMF, Vancouver, Canada. Private communication.

[97] R. Armenta. TWIST Magnet: Field Map Study (TN68). Technical report, TWIST collaboration, TRIUMF, 2002.

[98] A. Olin. T0 Wire Distortion. Internal TWIST report, July 2009.

[99] G. Marshall. OPERA map corrections from Hall and NMR maps at 2.0 T. Internal TWIST report, April 2009.

[100] R. Bayes. *Measurement of ρ (in preparation).* PhD thesis, University of Victoria, 2009.

[101] COMSOL. COMSOL Multiphysics. http://www.comsol.com.

[102] P. Depommier. TN96: Muon polarization in the $\pi^+ \to \mu^+\nu\gamma$ decay. Technical report, TWIST collaboration, TRIUMF, 2005.

[103] A. Grossheim. Decay of negative muons bound in ^{27}Al. Aug 2009. arXiv:hep-ex/0908.4270.

[104] H. Yukawa. On the Interaction of Elementary Particles. *I, Proc. Phys.-Math. Soc. Jpn.*, 17:48, 1935.

[105] C.D. Anderson and S.H. Neddermeyer. Cloud Chamber Observations of Cosmic Rays at 4300 Meters Elevation and Near Sea-Level. *Phys. Rev.*, 50:263–271, 1936.

[106] S.H. Neddermeyer and C.D. Anderson. Cosmic-Ray Particles of Intermediate Mass. *Phys. Rev.*, 54:88–89, 1938.

[107] S.H. Neddermeyer and C.D. Anderson. Nature of Cosmic-Ray Particles. *Rev. Mod. Phys.*, 11:191–207, 1939.

[108] M. Riordan. *The Hunting of the Quark*. Sage Publications, 1987.

[109] M. Conversi, E. Pancini and O. Piccioni. On the Disintegration of Negative Mesons. *Phys. Rev*, 71:209–210, 1947.

[110] E. Fermi, E. Teller and V. Weisskopf. The Decay of Negative Mesotrons in Matter. *Phys. Rev.*, 71:314–315, 1947.

[111] C.M.G. Lattes, G.P.S. Occhialini and C.F. Powell. Observations on the Tracks of Slow Mesons in Photographic Emulsions Part 1. *Nature*, 160:453–456, 1947.

[112] C.M.G. Lattes, G.P.S. Occhialini and C.F. Powell. Observations on the Tracks of Slow Mesons in Photographic Emulsions Part 1. *Nature*, 160:486–492, 1947.

[113] T.D. Lee. A Brief History of the Muon. *Hyperfine Interact.*, 86:439–453, 1994.

[114] C.S. Wu and V.W. Hughes. *Muon Physics: Introduction and History.* Academic Press Inc., 1977.

[115] R.A. Millikan. Mesotron as the Name of the New Particle. *Phys. Rev.*, 1:105, December 1938.

[116] C.D. Anderson and S.H. Neddermeyer. Mesotron (Intermediate Particle) as a Name for the New Particles of Intermediate Mass. *Nature*, 142:878, November 1938.

[117] H. Lyle. Anderson, Carl. Interview by Harriett Lyle. Oral History Project, California Institute of Technology. Retrieved April 2008 from the World Wide Web: `http://resolver.caltech.edu/CaltechOH:OH_Anderson_C`, 1979.

[118] A.H. Compton. Foreword: Symposium on Cosmic Rays. *Rev. Mod. Phys.*, 11:122, 1939.

[119] H.J. Bhabha. The Fundamental Length Introduced by the Theory of the Mesotron (Meson). *Nature*, 143:276–277, Feburary 1939.

[120] J. L. Beveridge *et al.* A spin rotator for surface μ^+ beams on the new M20 muon channel at TRIUMF. *Nucl. Instrum. Methods Phys. Res., Sect. A*, 240:316–322, 1985.

[121] Triumf CMMS. Helios superconducting solenoid. Website: `http://cmms.triumf.ca/equip/helios.html`.

[122] G. Morris, TRIUMF, Vancouver, Canada. Private communication.

[123] S.R. Dunsiger *et al.* Magnetic field dependence of muon spin relaxation in geometrically frustrated $Gd_2Ti_2O_7$. *Phys. Rev. B*, 73(172418), 2006.

[124] F. James. MINUIT – Function Minimization and Error Analysis, CERN Program Library Entry D 506.

[125] J.F. Ziegler. The stopping and range of ions in matter. http://www.srim.org/.

[126] TRIUMF CS. TRIUMF Computing Services description of SRIM. http://it-services.triumf.ca/scientific-computing/software/detector-engineering/srim-1.

[127] D.M. Garner. *Application of the muonium spin rotation technique to a study of the gas phase chemical kinetic of muonium reactions with the halogens and hydrogen halides.* PhD thesis, University of British Columbia, June 1979.

[128] J. Doornbos, TRIUMF, Vancouver, Canada. Private communication.